J.R. Serrano; Arnau Martínez, FJ.; Piqueras, P.; Reyes Belmonte, MA. (2011). Assessment of a methodology to mesh the spatial domain in the proximity of the boundary conditions for one-dimensional gas dynamic calculation. Mathematical and Computer Modelling. 54:1747-1752. doi:10.1016/j.mcm.2010.11.073

Assessment of a methodology to mesh the spatial domain in the proximity of the boundary conditions for one-dimensional gas dynamic calculation

J. R. Serrano, F. J. Arnau, P. Piqueras*, M. A. Reyes-Belmonte

Universidad Politécnica de Valencia, CMT-Motores Térmicos, Camino de Vera s/n, 46022 Valencia, Spain.

Abstract

Solution of governing equations for one-dimensional compressible unsteady flow has been performed traditionally using a homogenously distributed spatial mesh. In the resulting node structure, the internal nodes are solved by applying a shock capturing finite difference numerical method whereas the solution of the end nodes, which define the boundary conditions of the pipe, is undertaken by means of the Method of Characteristics. Besides the independent solution of every method, the coupling between the information obtained by the method of characteristics and the finite differences method is key in order to reach a good accuracy in gas dynamics modeling. The classical spatial mesh could provide numerical problems leading the boundary to generate mass, momentum and energy lack of conservation because of the interpolation methodology usually applied to draw the characteristics and path lines from its departure point at calculation time to the end of the pipe during the next time-step. To deal with these undesirable behavior, at this work a modification of the traditional grid including an extra node close to the boundary is proposed in order to explore its ability to provide numerical results with higher conservation fulfillment.

Keywords: gas dynamics, time-marching, mesh, boundary conditions

1. Introduction

The work reported in the present paper deals with the solution of the boundary conditions in gas dynamics codes and how the way in which the sort of spatial mesh of the 1D-elements can affect the accuracy of the solution. 1D-elements are those in which one of the spatial dimensions is higher than the others, so a length variable is necessary to define the element, as in pipes or ducts. Instead of the traditional mesh to discretize the 1D-elements which accounts for uniformly distributed nodes, the proposal of Corberán and Gascón [1] has been developed and implemented in OpenWAM^{TM}[2] [3], an open source code for gas dynamics calculation of one-dimensional compressible unsteady and non-homentropic flow developed at CMT-Motores Térmicos.

*P. Piqueras. CMT-Motores Térmicos, Universidad Politécnica de Valencia, Camino de Vera s/n, 46022 Valencia, Spain.
Phone: +34 963877650 Fax: +34 963877659 e-mail: pedpicab@mot.upv.es

January 9, 2018

According to this proposal, for a given spatial mesh size equal to Δx an extra node is added, so that the distance from the end nodes of a 1D-element to the neighboring ones is set to $\Delta x/2$ instead of Δx. As a consequence, when solving the neighboring nodes of the end of the 1D-element, the mass, momentum and energy fluxes are evaluated at the extremes of their control volume which coincides with the end of the 1D-element. This effect contributes to increase the accuracy of the solution obtained in the boundary conditions. The existance of contact dicontinuities in the boundary conditions between a 1D and 0D-elements is analyzed as a validation of the proposed methodology. 0D-elements are those in which all the geometrical parameters are similar and the volume is used to define the element. That situation is representative of intake and exhaust valves opening in internal combustion engines and its modelling is traditionally characterized by the lack of mass conservation in the solution of the governing equations [4] that can be mitigated with the proposed extra-node mesh.

2. Equations and mesh methodology

The governing equations for one-dimensional unsteady compressible non-homentropic flow, i.e. the mass, momentum and energy conservation equations [5] [6], form a hyperbolic system of partial differential equations in the form of equation 1. The vectors are represented in matrix form in equation 2.

$$\frac{\partial \mathbf{W}(x,t)}{\partial t} + \frac{\partial \mathbf{F}(\mathbf{W})}{\partial x} + \mathbf{C}(x,\mathbf{W}) = 0 \tag{1}$$

$$\begin{aligned} \mathbf{W}(x,t) &= \begin{bmatrix} \rho F \\ \rho u F \\ F\left(\rho\frac{u^2}{2} + \frac{p}{\gamma-1}\right) \end{bmatrix} \quad \mathbf{F}(\mathbf{W}) = \begin{bmatrix} \rho u F \\ \left(\rho u^2 + p\right) F \\ uF\left(\rho\frac{u^2}{2} + \frac{\gamma p}{\gamma-1}\right) \end{bmatrix} \\ \mathbf{C}(x,\mathbf{W}) &= \begin{bmatrix} 0 \\ -p\frac{dF}{dx} + g\rho F \\ -q\rho F \end{bmatrix} \end{aligned} \tag{2}$$

In equation 2, $\mathbf{W}$ represents the vector of flow properties or vector of solutions, $\mathbf{F}$ is the vector of fluxes (mass, momentum and energy) and vector $\mathbf{C}$ includes the source terms that take into account the effects of area changes, friction and heat transfer respectively. In that equation F represents the cross section-area of the 1D-element.

This system of equations is applied to the solution of flow advection through 1D-elements like ducts or channels. The solution of this problem requires the length of the element to be discretized into nodes of calculation where the conservation equations are solved. The flow properties at the internal nodes of the 1D-element are obtained applying a shock capturing numerical methods as proposed by Takizawa [7], Azuma [8] and Poloni [9].

For the solution of an internal node j at instant time $n+1$, point $(j, n+1)$, these methods evaluate the fluxes entering and exiting to/from the control volume, as shown in Figure 1(a) for the case of the two-step Lax-Wendroff method [10]. The calculation of these fluxes allows obtaining the solution of the flow properties at $(j, n+1)$ by solving the second step of the method, which is shown in equation 5. Equation 3 and 4 correspond to the first step of the two-step Lax-Wendroff method [11], which provides the solution at $(j-1/2, n+1/2)$ and $(j+1/2, n+1/2)$ from $(j-1, n)$ and (k, n) respectively [12] [13]. At these equations Δt is the time-step obtained from the application of CFL condition [14].

$$\mathbf{W}_{j-\frac{1}{2}}^{n+\frac{1}{2}} = \frac{1}{2}\left(\mathbf{W}_{j}^{n} + \mathbf{W}_{j-1}^{n}\right) - \frac{\Delta t}{2\Delta x}\left(\mathbf{F}_{j}^{n} - \mathbf{F}_{j-1}^{n}\right) - \frac{\Delta t}{4}\left(\mathbf{C}_{j}^{n} + \mathbf{C}_{j-1}^{n}\right) \tag{3}$$

$$\mathbf{W}_{j+\frac{1}{2}}^{n+\frac{1}{2}} = \frac{1}{2}\left(\mathbf{W}_{k}^{n} + \mathbf{W}_{j}^{n}\right) - \frac{\Delta t}{2\Delta x}\left(\mathbf{F}_{k}^{n} - \mathbf{F}_{j}^{n}\right) - \frac{\Delta t}{4}\left(\mathbf{C}_{k}^{n} + \mathbf{C}_{j}^{n}\right) \tag{4}$$

$$\mathbf{W}_{j}^{n+1} = \mathbf{W}_{j}^{n} - \frac{\Delta t}{\Delta x}\left(\mathbf{F}_{j+\frac{1}{2}}^{n+\frac{1}{2}} - \mathbf{F}_{j-\frac{1}{2}}^{n+\frac{1}{2}}\right) - \frac{\Delta t}{2}\left(\mathbf{C}_{j+\frac{1}{2}}^{n+\frac{1}{2}} + \mathbf{C}_{j-\frac{1}{2}}^{n+\frac{1}{2}}\right) \tag{5}$$

Figure 1

If the 1D-element is discretized with a homogeneously distributed spatial mesh, which is with the same size Δx between all the nodes, the end nodes can be solved by means of the Method of Characteristics [5]. By means of this method, the solution at the end node k at time level $n+1$ is obtained from the Riemman variables and the entropy level, so that their departure points have to be calculated at time level n. From these points the Riemman variables and the entropy level reach the end of the 1D-element at time level $n+1$. It allows the specific solution for the boundary condition. This procedure is sketched in Figure1(b). The values of the Riemman invariables and entropy level are known at the departure point values. However these values do not coincide with the values at point $(k, n+1)$ because of the influence of friction, heat transfer and area changes along the characteristic lines as expressed by means of equations 6 and 7 [5] [6].

$$\lambda = \lambda_{dp} + \delta\lambda_{friction} + \delta\lambda_{heat} + \delta\lambda_{area\_changes} \tag{6}$$

$$A_A = A_{A_{dp}} + \delta A_{A_{friction}} + \delta A_{A_{heat}} + \delta A_{A_{area\_changes}} \tag{7}$$

One of the problems of this sort of solution arises, on the one hand, from the high influence of the solution of the end node, of first order in time and space, on the solution of the neighboring nodes. On the other hand, the accurate solution in the internal nodes obtained by means of shock capturing methods is decoupled from the solution of the end nodes because of the interpolation process needed to evaluate the departure point and the value of the Riemann variables and the entropy level every time-step.

To avoid these problems and to obtain a higher accuracy in conservation of the flow properties, it is proposed an alternative methodology to mesh the spatial domain. According to this proposal the neighboring nodes of the 1D-element boundaries are placed at a distance $\Delta x/2$ of the end, while the rest of the internal nodes are separated a distance of Δx, as it is shown in Figure 2. With this procedure an extra node has been introduced with respect to the traditional homogeneously distributed mesh.

Figure 2

The solution of the neighboring node to the end of the 1D-element is shown in Figure 2(a). The flow properties at node j at time level $n+1$ are calculated again by applying the two-step Lax-Wendroff method, but now equation 4 to obtain the vector of fluxes at point $(k, n+1/2)$ is not necessary, due to the vector of fluxes is obtained by applying the method of characteristics. The departure point for the Riemman invariables and entropy level will be placed between nodes j and k. Once the vector of fluxes is known at nodes $(k, n+1/2)$ and $(j-1/2, n+1/2)$ the solution of flow properties is obtained applying the second step of the Lax-Wendroff method, equation 8.

$$\mathbf{W}_j^{n+1} = \mathbf{W}_j^n - \frac{\Delta t}{\Delta x}\left(\mathbf{F}_k^{n+\frac{1}{2}} - \mathbf{F}_{j-\frac{1}{2}}^{n+\frac{1}{2}}\right) - \frac{\Delta t}{2}\left(\mathbf{C}_k^{n+\frac{1}{2}} + \mathbf{C}_{j-\frac{1}{2}}^{n+\frac{1}{2}}\right) \tag{8}$$

The problem now is to obtain flow properties at the boundary node k at time level $n+1$. A first order method has been used to solve that boundary node.

$$\mathbf{W}_k^{n+1} = \mathbf{W}_k^{n+\frac{1}{2}} - \frac{\Delta t}{2\Delta x}\left(\mathbf{F}_k^{n+\frac{1}{2}} - \mathbf{F}_{j-\frac{1}{2}}^{n+\frac{1}{2}}\right) + \frac{\Delta t}{2}\mathbf{C}_k^{n+\frac{1}{2}} \tag{9}$$

According to equation 9 and Figure 2(b) the flow properties at point $(k, n+1)$ are calculated with the information of properties at point $(k, n+1/2)$, which are known from the solution of the Method of Characteristics, and at point $(j-1/2, n+1/2)$ whose properties are obtained from the first-step of the Lax-Wendroff method. Another feasible solution way will be to use the Method of Characteristics to obtain the flow properties at the boundary node $(k, n+1)$. In this case the departure points will be placed between points $(j-1, n)$ and (k, n).

3. Results and discussion

The proposed extra-node methodology has been applied to simulate the behavior of the flow for the model shown in Figure 3. This model consists of an intermediate volume of 1,000 cm^3 represented by the big square numbered as 1. It is coupled to two pipes of 30 mm in diameter, represented by dark lines in Figure 3. The pipe numbered as 1 represents the inlet duct which is 300 mm in length; the pipe numbered as 2 represents the outlet duct which is 200 mm in length. The small size squares represent the boundary conditions. In particular, boundary conditions 1 and 2 are the inlet and outlet boundary conditions to the volume respectively. The discharge coefficients at these boundaries are equal to 1. Boundary conditions 3 and 4 allow to impose the inlet and outlet pressure pulses to the system.

Figure 3

Sinusoidal pressure signals with phase-shift have been imposed at the inlet and outlet of the system to generate a thermal contact discontinuity at the inlet and outlet of the volume. The imposed pressure pulses are shown in Figure 4(a). The frequency is 50 Hz for both inlet and outlet pulses, but have different phase. The average pressure for the inlet pulse is 1.1 bar with 0.2 bar in amplitude. For the outlet pulse the average pressure is 1 bar with 0.3 bar in amplitude. The Figure 4(b) shows the instantaneous mass flow at the inlet and outlet of the volume by using the proposed extra-node methodology (dark color) and the traditional homogeneously distributed mesh (light color). The solid line represents the mass flow at the inlet node to volume and the dashed line plots the mass flow at the outlet one. The instantaneous negative values of mass flow points out the existance of back-flow through the volume.

Figure 4

When the converged solution is achieved, there should not be differences between the mass flow coming into and going out to the volume due to the fact that there is no mass accumulation at steady-state conditions and the volume is not a source generating or lossing mass. However, Table 1 shows a big unbalance in mass conservation at volume when the traditional mesh is applied. On the contrary, the proposed extra-node mesh shows negligible mass conservation errors. In both cases the mass conservation error has been calculated according to equation 10,

$$error\ (\%) = \frac{\sum_{i}^{N} (\dot{m}_{out_i} \cdot \Delta t_i) - \sum_{i}^{N} (\dot{m}_{in_i} \cdot \Delta t_i)}{\sum_{i}^{N} (\dot{m}_{in_i} \cdot \Delta t_i)} \tag{10}$$

where ṁ is the mass flow at the inlet or outlet node of the 1D-element, as defined, the subscript i represents every time level and N is the number of time-steps representing the duration of the inlet pulse, i.e. a cycle of calculation.

Table 1

Figure 5 represents the mass flow at every pipe boundary for both sort of 1D-elements mesh. The boundaries are located at 0 cm (first node of inlet pipe), 30 cm (2 nodes corresponding to the end of the inlet pipe and the beginning of the outlet pipe) and 50 cm (last node of the outlet pipe).

Figure 5

Figure 5(a) shows the obtained results when a coarse mesh is applied to both mesh methodologies. The traditional methodology does not work properly when few numbers of nodes are considered. Therefore the spatial mesh up to 1 cm has been necessary to obtain similar accuracy than the extra-node methodology working with a coarse mesh, as it is shown in Figure 5(b). In this case the artificial mass flow generation inside the volume is small for the traditional methodology although that mass conservation error is still lower with the extra-node mesh. In addition, the conservation of mass flow between the first and the last nodes of the model with the spatial mesh size of 1 cm using the traditional homogeneously distributed mesh is not as good as the obtained with the proposed methodology even with a more coarse mesh. The exact value of the mass flow variable for that model is 0.0553 kg/s.

Table 2 summarizes the information obtained with different sizes of spatial mesh applying the traditional methodology. The results are compared with that obtained when applying the extra-node mesh.

Table 2

The traditional methodology to mesh the 1D-elements needs a very thin spatial mesh size which means higher number of calculation nodes to provide a good accuracy in mass conservation. It results in a higher computational effort. However, the extra-node mesh methodology can be used with a coarse spatial mesh keeping good accuracy in mass flow conservation. Furthermore, it preserves the computational effort even in the case of complex flow conditions such as contact discontinuities existance. These situations in which a back flow through the system appears are very common during internal combustion engine operation as in the intake or exhaust cylinder valves opening. Therefore it is important to ensure the balance between the good accuracy in results and the lower computational effort.

The computational effort for the same spatial mesh size is higher with the proposed methodology than with the traditional one, due to the fact that it has been added an extra node. Therefore the number of times the conservation equations system are solved is increased. In addition, this extra node implies a modification of the time-step according to the CFL stability criterion [14], which becomes lightly reduced because of the smaller mesh at the boundaries $\Delta x/2$. Nevertheless, this increase of computational effort is compensated by the fact that the traditional mesh requires a very reduced spatial mesh size to ensure mass conservation.

4. Summary and conclusions

The solution of the governing equations for compressible flow in 1D-elements requires to divide the spatial domain into nodes where the conservation equations are solved. Traditionally, a homogeneously distributed spatial mesh has been used to define the calculation nodes, being Δx the distance between all the nodes. However, the use of this sort of spatial mesh can provide lack of mass conservation at boundaries, mainly if thermal contact discontinuities appears. To avoid that phenomenon it has been proposed an extra-node mesh. This method consists on placing the neighboring nodes to the boundary ones at a distance $\Delta x/2$, while all the other internal nodes are separated a distance equal to Δx. The use of this proposed mesh leads to solve the internal nodes defining control volumes covering all the length of the 1D-element, as in a finite volume discretization. Therefore, the solution provided by the Method of Characteristics at the boundaries is in accordance with the vector of fluxes applied in the solution of the neighboring node by means of shock capturing methods. Then there is no lack of information between the last control volume and the boundary condition, providing the proposed extra-node mesh a higher accuracy in mass flow conservation. It has been proved the better accuracy in mass conservation at pipe boundaries when the proposed extra-node mesh is used to simulate thermal contact discontinuities. To obtain a similar accuracy by using the traditional mesh it would be necessary to reduce dramatically the spatial mesh size, which would mean the need of higher computational effort.

[1] J.M. Corberán, L. Gascón, New method to calculate unsteady 1-D compressible flow in pipes with variable cross-section. Application to the calculation of the flow in intake and exhaust pipes of IC engines, Proceedings of the ASME Internal Combustion Engine Division Spring Meeting, ICE Engine Modeling, 23: 77–87,1995.

[2] J. Galindo, J.R. Serrano, F. Arnau, P. Piqueras, Description and analysis of a one-dimensional gas-dynamic model with Independent Time Discretization, Proceedings of the ASME Internal Combustion Engine Division 2008 Spring Technical Conference ICES2008, ICES2008-1610: 187–197, 2008.

[3] Openwam website. CMT-Motores Térmicos. Universidad Politécnica de Valencia. www.openwam.org.

[4] J.R. Serrano, F.J. Arnau, P. Piqueras, A. Onorati, G. Montenegro, 1D gas dynamics modelling of mass conservation in complex ducts engines with thermal discontinuities, Mathematical and Computer Modelling, 49: 1078–1088,2009.

[5] R.S. Benson, The Thermodynamics and Gas Dynamics of Internal Combustion Engines, Vol. 1, Oxford, Clarendon Press, 1982.

[6] D.E. Winterbone, R.J. Pearson, Theory of Engine Manifold Design: Wave Action Methods for IC Engines, London, Professional Engineering Publishing, 2000.

[7] M. Takizawa, T. Uno, T. Oue, T. Yura, A study of gas exchange process simulation of an automotive multi-cylinder internal combustion engine, SAE Technical Paper, 820410, 1982.

[8] T. Azuma, T. Yura, Y. Tokunaga, Some aspects of constant pressure turbocharged marine diesel engines of medium and low speed, Journal of Engineering for Power, 105: 697–711, 1983.

[9] M. Poloni, D.E. Winterbone, J.R. Nichols, Comparison of unsteady flow calculations in a pipe by the method of characteristics and the two-step differential Lax-Wendroff method, International Journal of Mechanical Science, 29: 367–378,1987.

[10] P.D. Lax, B. Wendroff, Systems of conservation laws, Communications on Pure and Applied Mathematics, 17: 381–398, 1964.

[11] R.D. Richtmyer, K.W. Morton, Difference Methods for Initial Value Problems, New York, Interscience Tracts in Pure and Applied Mathematics, 1967.

[12] S. Burstein, Finite difference calculations for hydrodynamic flows containing discontinuities, Journal of Computational Physics, 1: 198–222, 1967.

[13] E. Rubin, S. Burstein, Difference methods for the inviscid and viscous equations of compressible gas, Journal of Computational Physics, 2: 178–196, 1967.

[14] R. Courant, K.O. Friedrichs, H. Lewy, Über die partiellen Differenzengleichungen der mathematisches Physik (Text in German), Mathematische Annalen, 100: 32–74,1928.

NOTATION

0D	zero-dimensional
1D	one-dimensional
A_A	dimensionless entropy level
C	source term vector
CFL	Courant-Friedrich-Lewy criterion
F	cross-section area
F	flow term vector
g	friction term
$\dot{m}$	mass flow
p	gas pressure
q	heat per unit of time and area
t	time dimension
u	gas velocity
W	field variable vector
OpenWAM	Open source code Wave Action Model
x	axial dimension

Greek letters

$\delta\lambda$	variation of Riemann variable
Δt	time-step
Δx	mesh size
γ	specific heat ratio
λ	incident characteristic (Riemann variable)
ρ	gas density

Subscripts and superscripts

dp	characteristic line or pathline departure point
i	index identifying calculated time-step
j	index for internal calculation node
k	index for boundary calculation node
n	index for time level
N	number of time-steps in a calculation cycle

List of Tables

1 Mass error between inlet and outlet node of the volume. 9
2 Mass conservation error and computational effort as function of the spatial mesh size. 9

List of Figures

1 Time marching with a homogeneously distributed spatial mesh: a) solution of internal nodes; b) solution of boundary nodes. 10
2 Time marching with the proposed extra-node mesh: a) solution of internal nodes; b) solution of boundary nodes. 10

3 Analyzed model represented by OpenWAM interface. 10
4 a) Pressure pulses at pipe boundaries; b) Instantaneous mass flow at volume. . . . 11
5 Mass flow conservation: a) coarse mesh; b) thin mesh. 11

	traditional mesh	extra-node mesh
Mass error	13.18%	−0.16%

Table 1: Mass error between inlet and outlet node of the volume.

	Pipe Mesh [cm]		Number of nodes			
	Inlet	Outlet	Inlet	Outlet	time [-]	mass error [%]
Traditional	15	10	3	3	1.00	13.18
Traditional	10	10	4	3	1.17	2.63
Traditional	5	5	7	5	3.01	1.01
Traditional	2	2	16	11	6.76	0.87
Traditional	1	1	31	21	15.22	0.64
Extra-node	15	10	4	4	1.49	-0.16

Table 2: Mass conservation error and computational effort as function of the spatial mesh size.

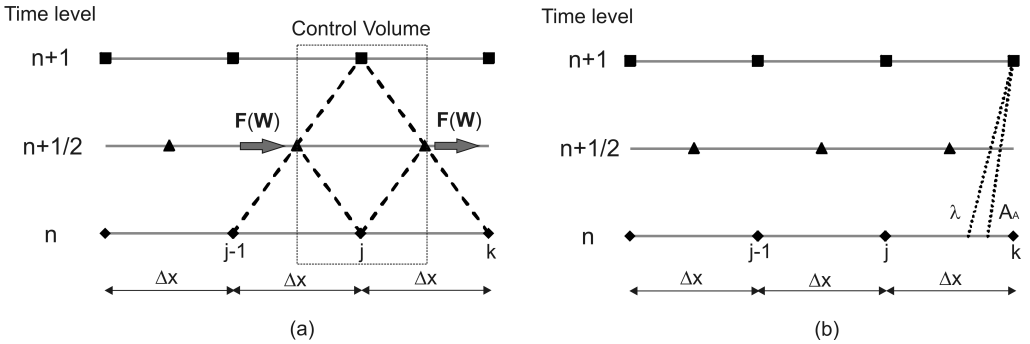

Figure 1: Time marching with a homogeneously distributed spatial mesh: a) solution of internal nodes; b) solution of boundary nodes.

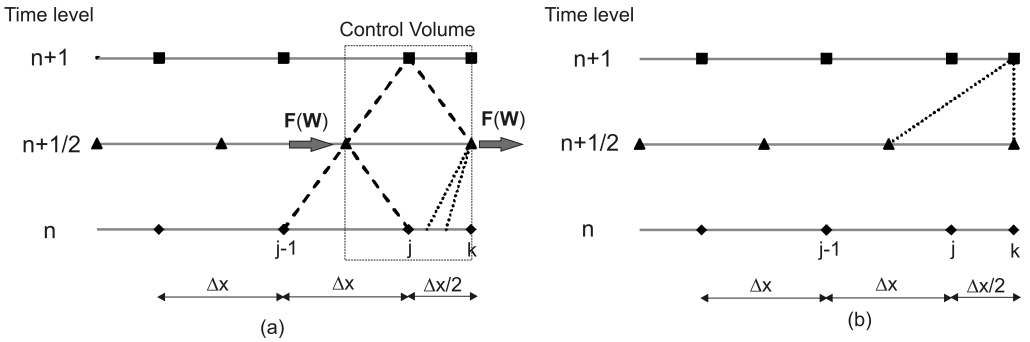

Figure 2: Time marching with the proposed extra-node mesh: a) solution of internal nodes; b) solution of boundary nodes.

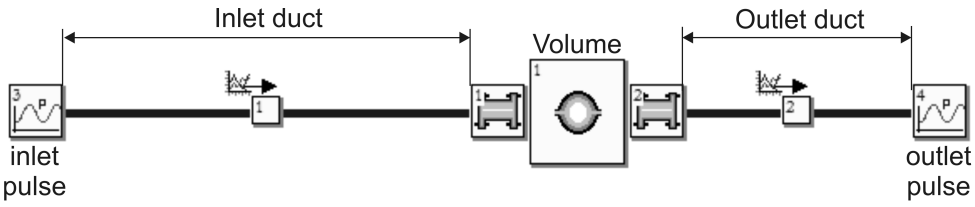

Figure 3: Analyzed model represented by OpenWAM interface.

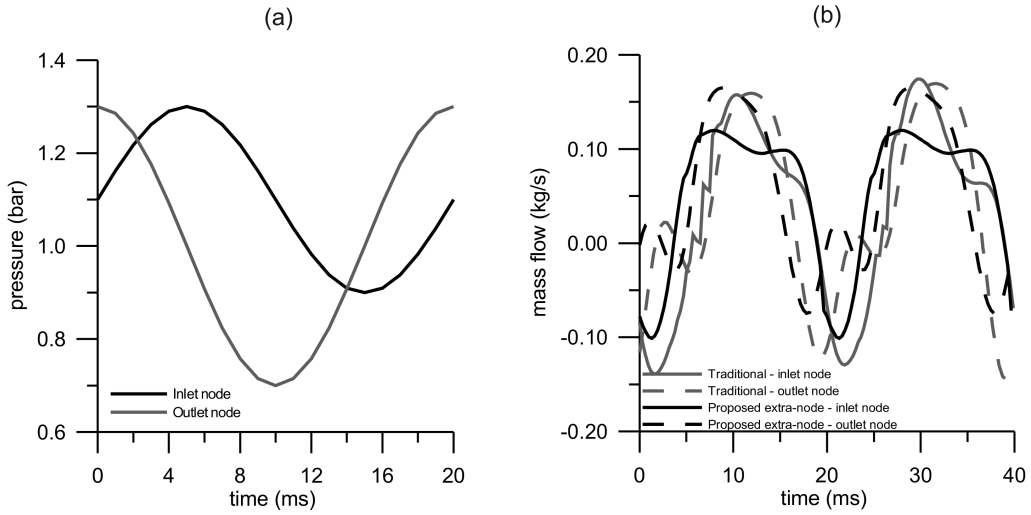

Figure 4: a) Pressure pulses at pipe boundaries; b) Instantaneous mass flow at volume.

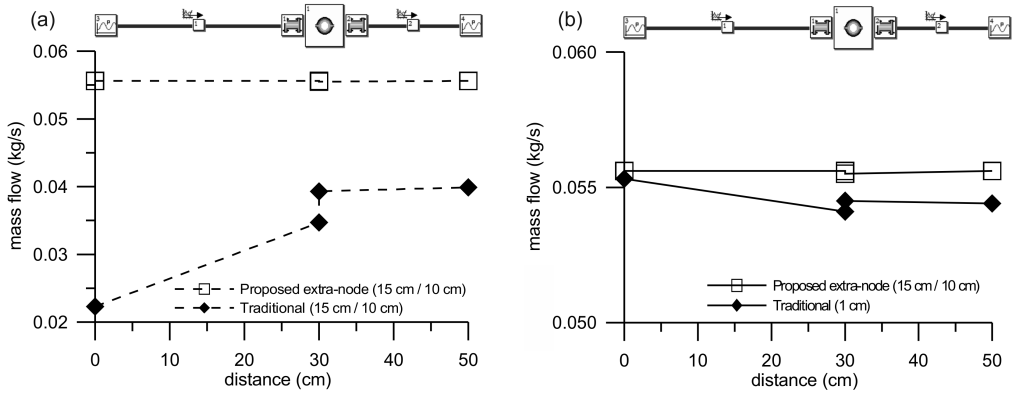

Figure 5: Mass flow conservation: a) coarse mesh; b) thin mesh.